WALAILAK JOURNAL
http://wjst.wu.ac.th Applied Mathematics

Thermal Performance of Convective-Radiative Heat Transfer in Porous Fins

Majid SHAHBABAEI[1,*] and Seyfollah SAEDODIN[2]

[1]*Faculty of Mechanical Engineering, Islamic Azad University, Shirgah Branch, Shirgah, Iran*
[2]*Faculty of Mechanical Engineering, Semnan University, Semnan, Iran*

([*]Corresponding author's e-mail: majid0123@gmail.com)

Received: 18 February 2013, Revised: 21 November 2013, Accepted: 28 December 2013

Abstract

Forced and natural convection in porous fins with convective coefficient at the tips under radiation and convection effects are investigated in this paper. Aluminum and copper as fin materials are investigated. In forced and natural convection, air and water are applied as working fluids, respectively. In order to solve this nonlinear equation, Homotopy Perturbation Method (HPM) and Variational Iteration Method (VIM) are used. To verify the accuracy of the methods, a comparison is made to the exact solution (BVP). In this work, the effects of porosity parameter (S_h), Radiation parameter (α) and Temperature-Ratio parameter (μ) on non-dimensional temperature distribution for both of the flows are shown. The results show that the effects of (α) and (μ) on temperature distribution in natural convection are based on porosity and in forced convection are uniform, approximately. Also, it is shown that both VIM and HPM are capable of being used to solve this nonlinear heat transfer equation.

Keywords: Forced convection, natural convection, porous fin, variational iteration method (VIM), homotopy perturbation method (HPM)

Nomenclature

Cp	Specific heat
Da	Darcy number, K/t2
G	gravity constant
Gr	Grashof number
k	Thermal conductivity
Kr	Thermal conductivity ratio, $\left(k_{eff} / k_f\right)$
K	Permeability of porous fin
L	Length
Nu	Nusselt number, $\left(hL / k_f\right)$
Pr	Prandtl number, $\left(\upsilon / \alpha\right)$
q	Heat transfer rate
Ra	Rayleigh number, Gr×Pr
$\widetilde{Ra}$	Modified-Darcy Rayleigh number
Sh	Porous parameter
T(x)	Temperature at any point
Tb	Temperature at fin base
t	Thickness of the fin
Bi	Biot Number, $\left(hL_c / k_b\right)$
$v_{W(x)}$	Velocity of fluid passing through the fin at any point

W	Width of the fin
x	Axial coordinate
X	Dimensionless axial coordinate, (x/L)
α	Radiation parameter
η	Temperature ratio parameter

Greek symbols

ϵ	Thermal diffusivity
β	Coefficient of volumetric thermal expansion
Δ	Temperature difference
φ	Porosity or void ratio
σ	Stephen-Boltzmann constant
θ	Dimensionless temperature
θb	Base temperature difference, (T_b-T_∞)
v	Kinematic viscosity
ρ	Density

Subscripts

s	Solid properties
f	Fluid properties
eff	Porous properties

Introduction

If the motion of a fluid arises from an external agent, or the motion of the heated object itself, which imparts pressure to drive the flow, the process is termed forced convection. If, on the other hand, no such externally induced flow exists, and the flow arises "naturally" from the effect of a density difference, resulting from a temperature or concentration difference in a body force field, such as gravity, the process is termed natural convection. In forced convection, externally imposed flow is generally known, whereas in natural convection it results from an interaction of the density difference with the gravitational field, and is therefore inevitably linked with and dependent on the temperature and/or concentration fields. In [2], the forced convection heat transfer in three-dimensional porous pin fin channels is numerically studied. The Forchheimer-Brinkman extended Darcy model and two-equation energy model are adopted to describe the flow and heat transfer in porous media. Air and water are employed as the cold fluids and the effects of the Reynolds number (Re), pore density (PPI) and pin fin form are studied in detail. The results show that, with proper selection of physical parameters, significant heat transfer enhancements and pressure drop reductions can be achieved simultaneously with porous pin fins, and the overall heat transfer performances in porous pin fin channels are much better than those in traditional solid pin fin channels. The effects of pore density are significant. As PPI increases, the pressure drops and heat fluxes in porous pin fin channels increase, while the overall heat transfer efficiencies decrease, and the maximal overall heat transfer efficiencies are obtained at PPI = 20 for both air and water. Furthermore, the effects of pin fin form are also remarkable. With the same physical parameters, the overall heat transfer efficiencies in long elliptic porous pin fin channels are the highest, while they are the lowest in short elliptic porous pin fin channels. In [3], a numerical analysis was performed to investigate the effects of fin location on to the bottom wall of a triangular enclosure filled with porous media whose height base ratio is 1. The temperature of the bottom wall was higher than that of the inclined wall while the vertical wall was insulated. Thus, the fin divides the heated bottom wall into 2 separate regions. The finite difference method was applied to solve the governing equations, which were written using the Darcy method. Solutions of algebraic equations were made by using the Successive Under Relaxation (SUR) technique.

The effective parameters on flow and temperature fields are: the Rayleigh number, location center of fin, non-dimensional fin height, and non-dimensional fin width. The obtained results indicated that the fin can be used as a control element for heat transfer and fluid flow. The effect of thermal radiation on the natural convection flow along a uniformly heated vertical porous plate with variable viscosity and uniform suction velocity was numerically investigated in [4]. The fluid considered in that study was of an optically dense viscous incompressible fluid of temperature-dependent viscosity. The laminar boundary layer equations governing the flow were shown to be non-similar. The governing equations were analyzed using a variety of methods: (i) a series solution for small values of ξ (a scaled stream wise coordinate depending on the transpiration); (ii) an asymptotic solution for large values of ξ ; and (iii) a full numerical solution using the Keller box method. The solutions were expressed in terms of the local shear stress and the local heat transfer rate. The working fluid was taken to have a Prandtl number Pr = 1, and the effects of varying the viscosity variation parameter, γ, the radiation parameter, Rd, and the surface temperature parameter, θw, were discussed. [5] conducted thermal analysis of natural convection porous fins. They grouped all the geometric and flow parameters that influence the temperature distribution into one parameter called Sh. Three cases of fin types were considered: the infinite fin, finite fin with insulated tip, and finite fin with uninsulated tip. Further investigation of Sh effect for all cases revealed that increasing Sh by increasing either Da or Ra increased the heat transfer from the fin. They also found that there is a limit to increasing both Kr and L/t that affect the heat transfer rate from the porous fin. [6] compared the heat transfer rates from convecting-radiating fins for different profile shapes. They used a finite difference approach to study this performance. They used rectangular, trapezoidal, triangular and concave parabolic shapes to compare heat transfer rates. The homotopy perturbation method (HPM) and variational iteration method (VIM) are the most well-known methods used to solve nonlinear equations. VIM and HPM were first introduced by Professor He. These methods can be applied successfully to various types of ordinary and partial differential equations. [8-10,13,14] developed VIM for solving linear and nonlinear problems, which arise in different branches of pure and applied sciences. Also, [11,12] introduced HPM, which is developed by combining the standard homotopy and perturbation method.

Materials and methods

Forced convection

The newer result obtained for heat transfer through porous media refer to forced and natural convection. The following results listed refer to a uniform unidirectional seepage flow through a homogeneous and isotropic porous medium. They are based on the idealization that the solid and fluid phases are found locally in thermal equilibrium. Hence, from [1] we have;

$$\overline{\mathrm{Nu}_L}=\frac{q''}{\overline{T}_w-T_\infty}\frac{L}{k_{eff}}=1.128\mathrm{Pe}_l^{\frac{1}{2}} \tag{1}$$

where $\overline{Nu_l}$ is the mean Nusselt Number, i.e. $\overline{h}l/k_{eff}$, $\overline{h}$ the mean heat transfer coefficient, k_{eff} the effective thermal conductivity of the porous fin, Pe_l the Peclet Number based on the overall longitudinal position, and $Pe_l = ul/\varphi_{eff}$, q'', $\overline{T}_w$ and T_∞ are heat flux , fin temperature and surrounding temperature.

Natural convection

In natural convection, the body force is due to internal density differences that are induced by heating or cooling effects. We assume that density and temperature changes are sufficiently small. Hence, from [1], we have;

$$\overline{Nu_L} = \frac{q''}{T_w - T_\infty} \frac{L}{k_{eff}} = 0.888 Ra_l^{\frac{1}{2}} \tag{2}$$

where $\overline{Nu_L}$ is the mean Nusselt Number based on the plate length L and Ra_l^* is the Darcy-modified Rayleigh number based on L. The q'', $\overline{T}_w$ and T_∞ are respectively heat flux, fin temperature and surrounding temperature. The Darcy-modified Rayleigh number is;

$$Ra_l^* = \frac{g\beta K(T_w - T_\infty)L}{\varphi_{eff} v_f} \tag{3}$$

Problem description

As shown in **Figure 1**, a rectangular fin profile is considered. The dimensions of the fin are length L, width W, and thickness t. The cross section area of the fin is constant. This fin is porous to allow the flow of infiltrate through it.

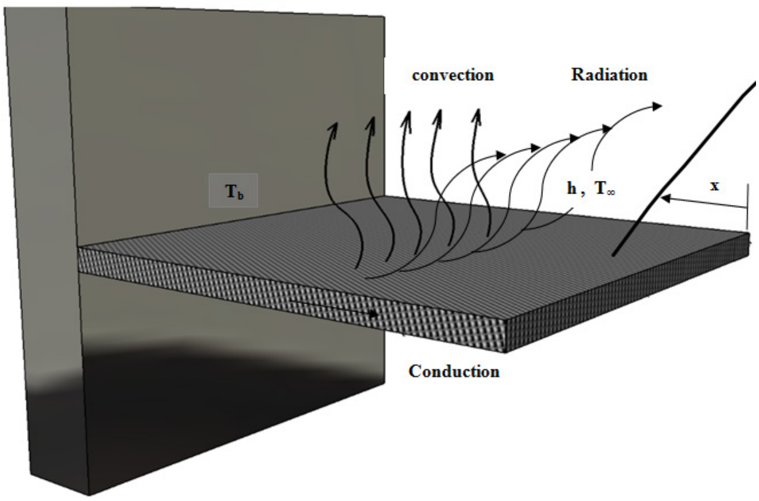

Figure 1 Schematic diagram of fin profile under consideration.

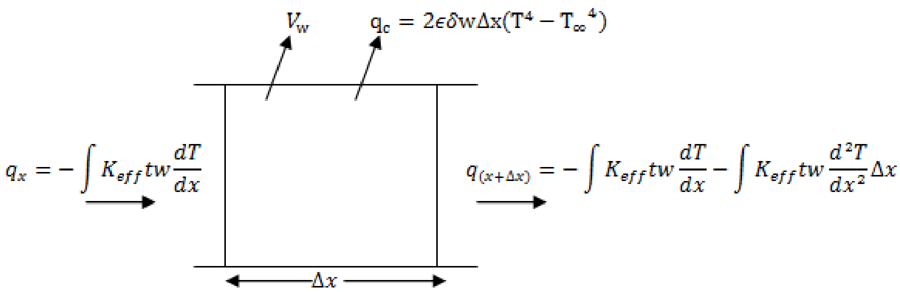

Figure 2 Energy balance in fin profile.

Now applying energy balance equation at steady state condition, as shown in **Figure 2**, we have;

$$-\int k_{eff} tw \frac{dT}{dX} + \int k_{eff} tw \frac{dT}{dX} + \int k_{eff} tw \frac{d^2T}{dX^2} \Delta x - \dot{m} C_p (T-T_\infty) - 2\sigma\varepsilon\Delta x (T^4 - T_\infty{}^4) = 0 \tag{4}$$

where $\dot{m} = \rho w \Delta x V_w$ and $A = w.\Delta x$.
From the Darcy model we have;

$$V_w = \frac{gK\beta}{v}\left(T - T_\infty\right) \tag{5}$$

Therefore, the energy balance at steady state becomes;

$$-\int k_{eff} tw \frac{dT}{dX} + \int k_{eff} tw \frac{dT}{dX} + \int k_{eff} tw \frac{d^2T}{dX^2} \Delta x - \left[\rho w \Delta x \frac{gK\beta}{v} C_p (T-T_\infty)\right] - 2\sigma\varepsilon\Delta x (T^4 - T_\infty{}^4) = 0$$

That is;

$$\frac{d^2T}{dx^2} - \rho \frac{gK\beta}{v k_{eff} t} C_p \left(T - T_\infty\right)^2 - \frac{2\sigma \in}{k_{eff} t}\left(T^4 - T_\infty^4\right) = 0 \tag{6}$$

We define the following dimensionless variables;

$$\xi = \frac{X}{L} \quad \theta = \frac{T - T_\infty}{T_b - T_\infty} \tag{7}$$

By substituting the dimensionless variables defined in Eq. (7), into Eq. (6), we have;

$$\frac{d^2\theta}{d\xi^2} - \frac{l^2}{\Delta t}\left(\Delta t\right)^2 \rho \frac{gK\beta}{v k_{eff} t} C_p \theta^2 - \frac{2\sigma \in}{k_{eff} t}\frac{l^2}{\Delta t}\left(\Delta t\right)^4 \left[\left[\theta + \eta\right]^4 - \eta^4\right] = 0$$

where

$$\eta = \frac{T_\infty}{\left[T_b - T_\infty\right]}, \; S_h = \frac{DaxRa}{k_r}\left(\frac{L}{t}\right)^2, \; \alpha = \frac{2\sigma \in}{kt} L^2 \left(\Delta T\right)^3$$

Hence, the governing equation may be written as;

$$\frac{d^2\theta}{dx^2} - S_h \theta(x)^2 - \alpha\left[\left(\theta(x) + \eta\right)^4 - \eta^4\right] = 0 \tag{8}$$

where α is the Radiation parameter, η is the Temperature-Ratio parameter and S_h is the Porosity parameter. Here is the summary of cases to be considered for this research;
Finite length fin with known convective coefficient at the tip;

$$\theta(0)=1,\left(\frac{d\theta}{dx}\right)_{x=1}+Biot.\theta(1)=0 \tag{9}$$

We have introduced this initial condition because of its Biot number. One of the important parameters to consider in forced and natural convection in heat transfer problems is the Biot number. It is found out that high and low Biot numbers belong to the forced and natural convection, respectively. So, the Biot number in the initial condition (9) will affect temperature distribution in forced and natural convection, and better shows the temperature distribution trend.

Analytical methods

Variational iteration method (VIM)

To explain the basic idea of VIM, consider the following nonlinear differential equation;

$$\mathrm{L}(\mathrm{u})+\mathrm{N}(\mathrm{u})=\mathrm{g}(\mathrm{x}) \tag{10}$$

where L is a linear operator, N is a nonlinear operator, and g(x) is an inhomogeneous term. According to the VIM, we can construct a correction functional as follows;

$$\theta_{n+1}(x)=\theta_n(x)+\int_0^x \lambda(\xi)[L\theta_n(\xi)+N\bar{\theta}_n(\xi)-g(\xi)]d\xi \tag{11}$$

where $\lambda(\xi)$ is a general Lagrangian multiplier which can be identified optimally via the VIM. The subscript *n* denotes the *n*th approximation, and $\tilde{u}$ is considered as a restricted variation, i.e. $\delta\tilde{u}_n = 0$.

Homotopy perturbation method (HPM)

To illustrate the basic ideas of this method, we consider the following equation;

$$A(F)-f(r)=0 \qquad r\in\Omega \tag{12}$$

with the boundary condition of;

$$B(F,\frac{\partial F}{\partial n})=0 \tag{13}$$

where A is a general differential operator, B a boundary operator, f (r) a known analytical function and Γ is the boundary of the domain Ω. A can be divided into 2 parts, which are L and N, where L is linear and N is nonlinear. Eq. (12) can therefore be rewritten as follows;

$$L(F)+N(F)-f(r)=0 \qquad r\in\Omega \tag{14}$$

Homotopy perturbation structure is shown as follows;

$$H(V,P)=(1-P)[L(V)-L(u_0)]+P[A(V)-f(r)]=0 \tag{15}$$

where

$$V(r,P) = \Omega \times [0,1] \to R \tag{16}$$

In Eq. (16), $p\epsilon[1,0]$ is an embedding parameter and u_0 is the first approximation that satisfies the boundary condition. We can assume that the solution of Eq. (8) can be written as a power series in p, as follows;

$$V = V_0 + PV_1 + ... = \sum_{i=0}^{n} V_i P^i \tag{17}$$

and the best approximation for solution is;

$$F = Lim_{p\to 1} V = V_0 + V_1 + ... \tag{18}$$

Fin temperature distribution

VIM approach

Its correction variational functional in θ can be expressed, respectively, as follow;

$$\theta_{n+1}(x) = \theta_n(x) + \int_0^x \lambda[\frac{d^2\theta_n(t)}{dt^2} - (S_h + 6\alpha\eta^2)\theta_n(t)^2 - \alpha\theta_n(t)^4 - 4\alpha\eta\theta_n(t)^3 - 4\alpha\eta^3\theta_n(t)]dt \tag{19}$$

where λ is Lagrange multiplier. The Lagrange multiplier can be identified as;

$$\lambda = \frac{1}{4\eta\sqrt{\alpha\eta}}(\exp^{2\eta\sqrt{\alpha\eta}(t-x)} - \exp^{-2\eta\sqrt{\alpha\eta}(t-x)}) \tag{20}$$

and the following variational iteration formula can be obtained by:

$$\theta_{n+1}(x) = \theta_n(x) + \int_0^x (\frac{1}{4\eta\sqrt{\alpha\eta}}(\exp^{2\eta\sqrt{\alpha\eta}(t-x)} - \exp^{-2\eta\sqrt{\alpha\eta}(t-x)}))[\frac{d^2\theta_n(t)}{dt^2} \\ - (S_h + 6\alpha\eta^2)\theta_n(t)^2 - \alpha\theta_n(t)^4 - 4\alpha\eta\theta_n(t)^3 - 4\alpha\eta^3\theta_n(t)]dt \tag{21}$$

We start with an arbitrary initial approximation that satisfies the initial condition, and, by substituting an arbitrary initial approximation in to Eq. (21), and after simplification, we have;

$$\theta_0(x) = \frac{(10\eta^{\frac{3}{2}}\sqrt{\alpha}-3)e^{2\eta^{\frac{3}{2}}\sqrt{\alpha}x}}{10\eta^{3/2}\sqrt{\alpha}(e^{\eta^{\frac{3}{2}}\sqrt{\alpha}})^4+10\eta^{\frac{3}{2}}\sqrt{\alpha}+3(e^{\eta^{\frac{3}{2}}\sqrt{\alpha}})^4-3} + \\ \frac{(e^{\eta^{\frac{3}{2}}\sqrt{\alpha}})^4(10\eta^{\frac{3}{2}}\sqrt{\alpha}+3)e^{-2\eta^{\frac{3}{2}}\sqrt{\alpha}x}}{10\eta^{3/2}\sqrt{\alpha}(e^{\eta^{\frac{3}{2}}\sqrt{\alpha}})^4+10\eta^{\frac{3}{2}}\sqrt{\alpha}+3(e^{\eta^{\frac{3}{2}}\sqrt{\alpha}})^4-3} \tag{22}$$

$$\theta_1(x) = \frac{(e^{\sqrt{55}})^{\frac{1}{5}}(\sqrt{55}+6)e^{-\frac{1}{10}\sqrt{55}x}}{\sqrt{55}(e^{\sqrt{55}})^{\frac{1}{5}}+\sqrt{55}+6(e^{\sqrt{55}})^{\frac{1}{5}}-6}$$
$$-2.993711028.10^{-7}e^{0.7416198487x} -$$
$$0.0000747350836e^{0.7416198487x+2.966479395} - \tag{23}$$
$$0.00241189105e^{5.932958790+0.7416198487x} +$$
$$2.291949871.10^{-8}e^{2.224859546x+1.483239697} -$$
$$0.000001999707645e^{-0.020000x} + ...$$

HPM approach

Now, we apply the HPM to Eq. (8). After separating the linear and nonlinear parts, we have;

$$H(\theta,P) = (1-P)[\frac{d^2\theta(x)}{dx^2} - 4\alpha\eta^3\theta(x)] + P[\frac{d^2\theta(x)}{dx^2} - (S_h + 6\alpha\eta^2)\theta(x)^2 - \alpha\theta(x)^4$$
$$-4\alpha\eta\theta(x)^3 - 4\alpha\eta^3\theta(x)] \tag{24}$$

After rearranging the above equation based on powers of P-terms, we have;

$$P^0 : \frac{d^2}{dx^2}\theta_0(x) + 4\eta^4 = 0,$$
$$\theta_0(0) = 1, \ \left(\frac{d}{dx}\theta_0(1)\right) + Biot.\theta_0(1) = 0 \tag{25}$$

$$P^1 : \frac{d^2}{dx^2}\theta_1(x) - (S_h + 6\eta^2\alpha)\theta_0(x)^2 - 4\theta_0(x)^3\eta\alpha - 4\theta_0(x)\eta^3\alpha - \theta_0(x)^4\alpha - \eta^4 = 0 \tag{26}$$
$$\theta_1(0) = 0, \ \left(\frac{d}{dx}\theta_1(1)\right) + Biot.\theta_1(1) = 0$$

By solving Eqs. (25) - (26) and after simplification, we have;

$$\theta_0(x) = \frac{(10\eta^{\frac{3}{2}}\sqrt{\alpha}-3)e^{2\eta^{\frac{3}{2}}\sqrt{\alpha}x}}{10\eta^{3/2}\sqrt{\alpha}(e^{\eta^{\frac{3}{2}}\sqrt{\alpha}})^4 + 10\eta^{\frac{3}{2}}\sqrt{\alpha} + 3(e^{\eta^{\frac{3}{2}}\sqrt{\alpha}})^4 - 3} +$$
$$\frac{(e^{\eta^{\frac{3}{2}}\sqrt{\alpha}})^4(10\eta^{\frac{3}{2}}\sqrt{\alpha}+3)e^{-2\eta^{\frac{3}{2}}\sqrt{\alpha}x}}{10\eta^{3/2}\sqrt{\alpha}(e^{\eta^{\frac{3}{2}}\sqrt{\alpha}})^4 + 10\eta^{\frac{3}{2}}\sqrt{\alpha} + 3(e^{\eta^{\frac{3}{2}}\sqrt{\alpha}})^4 - 3} \tag{27}$$

$$
\begin{aligned}
\theta_1(x) = &-\frac{1}{408148064958572078886426888209}\cdot\frac{1}{\cosh(\frac{1}{50})+30\sinh(\frac{1}{50})}\cdot \\
&(e^{\frac{1}{50}x}(161674950900374835212229917334\sin\left(\frac{17026949}{39062500}\right)- \\
&1640032976634118859790639065265\sin\left(\frac{17026949}{9765625}\right)+ \\
&627442167003018399422779587564\sin\left(\frac{17026949}{19531250}\right)+ \\
&594140176684806915108144256901\sin\left(\frac{51080847}{39062500}\right)+.....
\end{aligned}
\tag{28}
$$

Results and discussions

Figure 3a shows the non-dimensional temperature distribution in Al and Cu porous fins in forced convection by HPM and VIM, and compared with exact solutions in α = η = 0.1, air working fluid with u = 25 m/s, and different Biot numbers. Al and Cu Biot numbers are 1.4 and 1, respectively. From this figure, we can see that, by increasing the porosity parameter (S_h) the curve slope of the non-dimensional temperature distribution will increase; consequently, the fin quickly reaches the surrounding temperature and cools down rapidly. Increasing S_h can be accomplished by increasing Da, Ra, or L/t, or by decreasing Kr. From the viewpoint of analytical solution, both of the 2 methods are capable of solving the radiation-convection heat transfer equation in porous fins. Finally, the comparison with exact solution reveals that both the HPM and VIM are remarkably effective for solving these kinds of nonlinear problems.

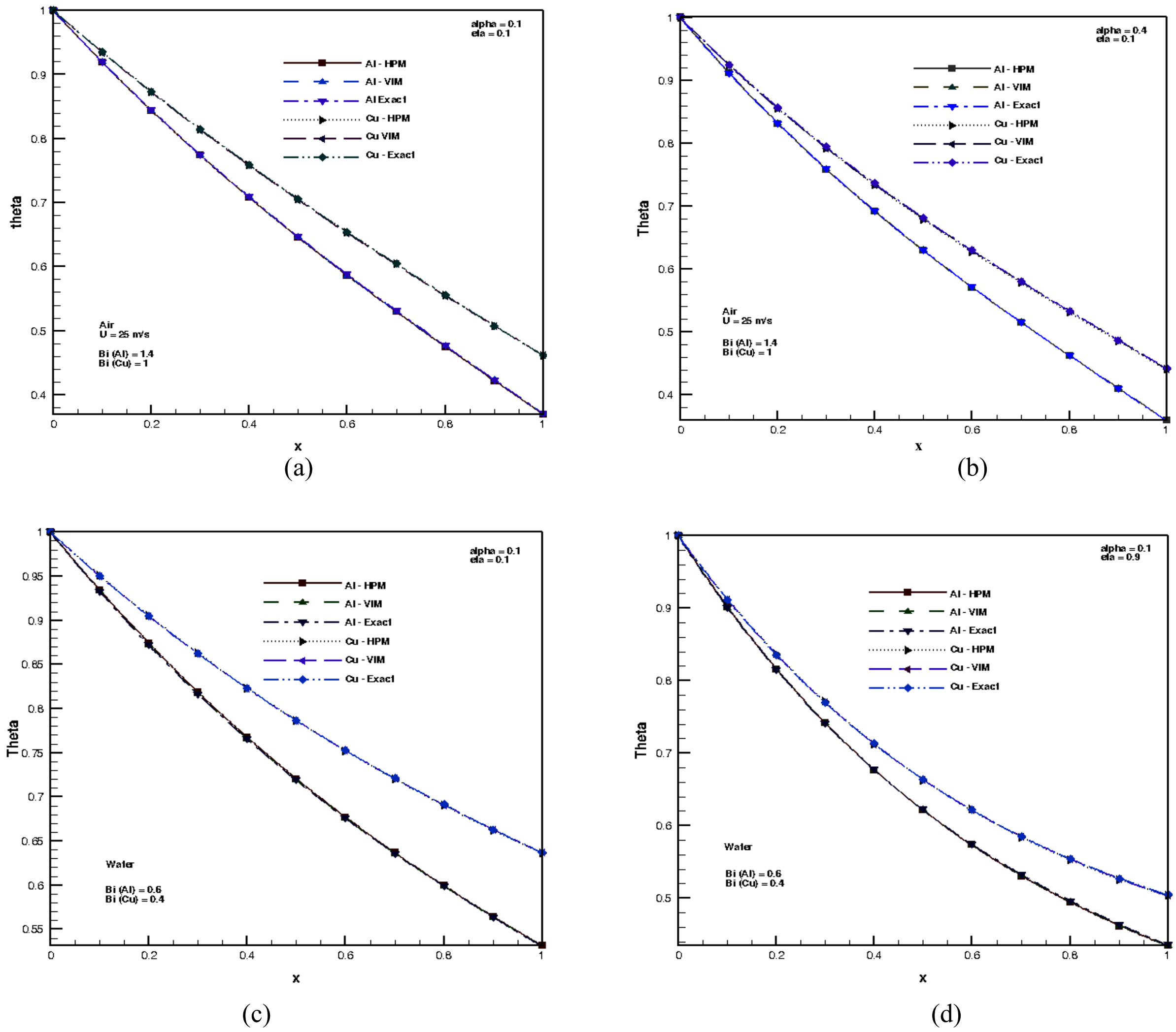

Figure 3 Comparison between HPM and VIM and exact solutions for along the Al and Cu porous fins with known convective coefficient at the tip in (a)(b) forced convection and (c)(d) natural convection.

Al and Cu Biot numbers are 1.4 and 1, respectively. From these figures, we can see the accuracy of the methods. Also, it is observed that the fin tip reaches the surrounding temperature faster as the value of Biot number increases. **Figure 3b** shows the comparison between non-dimensional temperature distribution in Al and Cu porous fins in forced convection by HPM and VIM , and their comparison with exact solutions in air working fluid with u = 25 m/s and different Biot numbers with $\alpha = 0.4$, $\eta = 0.1$. **Figure 3c** shows the comparison between non-dimensional temperature distribution in Al and Cu porous fins in natural convection by HPM and VIM , and their comparison with exact solutions in water working fluid and different Biot numbers with $\alpha = \eta = 0.1$. In this case, the Al and Cu Biot numbers are 0.6 and 0.4, respectively. **Figure 3d** shows the comparison between non-dimensional temperature distribution in Al and Cu porous fins in natural convection by HPM and VIM, and their comparison with exact solutions in water working fluid and different Biot numbers with $\alpha = 0.1$, $\eta = 0.9$. The Al and Cu Biot numbers are

0.6 and 0.4, respectively. From these figures, we can see the accuracy of the methods for solving these kinds of equations.

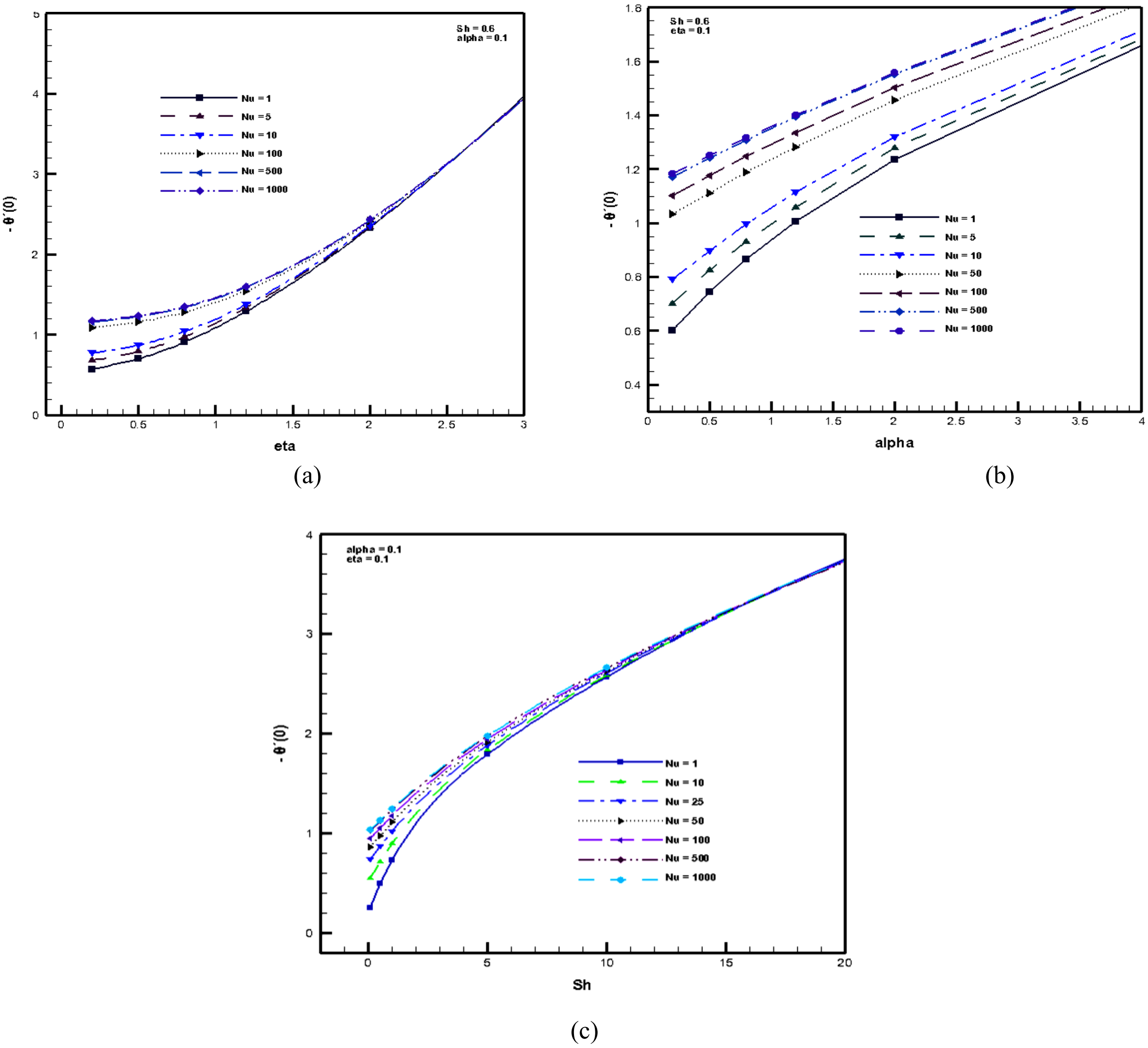

Figure 4 The variation of temperature gradient at the base of Al and Cu porous fins with the variation of η (a) and α (b) and S_h(c) at different values of Nu in forced and natural convection.

Also, it is observed that the fin tip reaches the surrounding temperature faster as the value of Biot number increases. **Figure 4a** shows the variation of temperature gradient at the base of Al and Cu porous fins with the variation of η at different values of Nu at the fin tip. In this case, S_h and α are 0.6 and 0.1, respectively. From this figure, we can see, by increasing of Nu number, the effect of temperature-ratio parameter on temperature gradient at the base of the fin will decrease. Also, it shows that the effect of temperature parameter on temperature gradient is limited to low values of it. **Figure 4b** shows the variation of temperature gradient at the base of Al and Cu porous fins with the variation of α at different values of Nu at the fin tip. The lower Nu numbers are related to natural convection and the upper Nu numbers are related to forced convection. From this figure, we can see that by increasing α, the temperature gradient at the base of the fins will increase. Also, it reveals that the effect of α on temperature gradient at the base of the fins is limited to low values of Nu. Hence, in high Nu numbers in forced convection, the effect of the radiation parameter is not significant. **Figure 4c** shows the variation of temperature gradient at the base of Al and Cu porous fins with the variation of S_h at different values of Nu at the fin tip. The lower Nu numbers are related to natural convection and the upper Nu numbers are related to forced convection. It is clear that the effect of Nu is limited to low values of S_h, where increasing Nu draws more heat from the fin base. However, at large values of S_h, increasing Nu has no significant influence on the heat transfer from the fin. This is simply because, as S_h increases, the temperature at the fin tip reaches the ambient temperature of the surrounding fluid, and thus the driving force for heat transfer from the fin tip reduces. This leads to a significant reduction from the use of high values of Nu at the tip.

Conclusions

In this paper aimed at solving the nonlinear radiation-convection heat transfer equation in porous fins, HPM and VIM have been used. Also, the forced and natural convections in porous fins have been investigated. Aluminum and copper as fin materials have been investigated. In forced convection, air with u = 25 m/s, and in natural convection, water, are used as working fluids. For studying the accuracy of the solutions, numerical analysis, named the Boundary Value Problem (BVP), has been used. In this work, the effects of porosity parameter (S_h), Radiation parameter (α) and Temperature-Ratio parameter (μ) on non-dimensional temperature distribution for both of two flows have been shown. Through observation of the figures, it is clear that by increasing the Nu number, the effect of radiation parameter on temperature gradient at the base of the fin will decrease in forced convection. Hence, in high Nu numbers in forced convection, the effect of radiation parameter is not significant. From the figures, we can see that in forced convection, the effect of temperature-ratio parameter on temperature gradient of the base of the fin is limited to low values of Nu. From the figures, it is clear that the effect of Nu is limited to low values of S_h, where increasing Nu draws more heat from the fin base. But at large values of S_h, increasing Nu has no significant influence on the heat transfer from the fin. This is simply because, as S_h increases, the temperature at the fin tip reaches the ambient temperature of the surrounding fluid, and thus the driving force for heat transfer from the fin tip reduces. This leads to a significant reduction from the use of high values of Nu at the tip. From the viewpoint of analytical methods, both VIM and HPM are capable of being used to solve the nonlinear Convection-Radiation heat transfer equation in porous fins. Finally, comparing with the exact solution (BVP), it is clear that the homotopy perturbation method and variational iteration method are remarkably effective for solving these kinds of nonlinear problems.

References

[1] PH Oosthuizen and D Naylor. *An Introduction to Convection Heat Transfer Analysis*. McGraw-Hill, New York, 1999.
[2] J Yang, M Zeng, Q Wang and A Nakayama. Forced convection heat transfer enhancement by porous fins in rectangular channels. *J. Heat Tran*. 2010; **132**, Article ID 051702.
[3] Y Varol, H Oztop and A Varol. Natural convection in porous triangular enclosures with a solid adiabatic fin attached to the horizontal wall. *Int. Comm. Heat Mass Tran*. 2007; **34**, 19-27.
[4] K Vafai, K Khanafer and MA Hossain. The effect of radiation on free convection flow of fluid with variable viscosity from a porous vertical plate. *Int. J. Therm. Sci.* 2001; **40**, 115-24.
[5] S Kiwan and MA Al-Nmir. Using porous fins for heat transfer enhancement. *J. Heat Tran.* 2001; **123**, 790-5.
[6] A Nguyen and A Aziz. The heat transfer rates from convecting-radiating fins for different profile shapes. *J. Heat Mass Tran.* 1992; **27**, 67-72.

[8] JH He. Approximate analytical solution for seepage flow with fractional derivatives in porous media. *Comput. Meth. Appl. Mech. Eng*. 1998; **167**, 57-68.
[9] JH He. Variational iteration method -a kind of non-linear analytical technique: Some examples. *Int. J. Nonlinear Mech.* 1999; **34**, 699-708.
[10] JH He and XH Wu. Variational iteration method: new development and applications. *Comput. Math. Appl*. 2007; **54**, 881-94.
[11] JH He. Homotopy perturbation technique. *Comput. Meth. Appl. Mech. Eng.* 1999; **178**, 257-62.
[12] JH He. Homotopy perturbation method: A new nonlinear analytical technique. *Appl. Math. Comput.* 2002; **135**, 73-9.
[13] G Shimin, M Liquan, Y Fang and Q Zhiyu. Compacton and solitary pattern solutions for nonlinear dispersive KdV-type equations involving Jumarie's fractional derivative. *Phys. Lett. A* 2012; **376**, 158-64.
[14] G Shimin and M Liquan. The fractional variational iteration method using He's polynomials. *Phys. Lett. A* 2011; **375**, 309-13.